

Photochemical & Photobiological Sciences

An international journal

Accepted Manuscript

This article can be cited before page numbers have been issued, to do this please use: A. Bhattacharyya, S. C. Makhal and N. Guchhait, *Photochem. Photobiol. Sci.*, 2019, DOI: 10.1039/C9PP00108E.



This is an Accepted Manuscript, which has been through the Royal Society of Chemistry peer review process and has been accepted for publication.

Accepted Manuscripts are published online shortly after acceptance, before technical editing, formatting and proof reading. Using this free service, authors can make their results available to the community, in citable form, before we publish the edited article. We will replace this Accepted Manuscript with the edited and formatted Advance Article as soon as it is available.

You can find more information about Accepted Manuscripts in the [Information for Authors](#).

Please note that technical editing may introduce minor changes to the text and/or graphics, which may alter content. The journal's standard [Terms & Conditions](#) and the [Ethical guidelines](#) still apply. In no event shall the Royal Society of Chemistry be held responsible for any errors or omissions in this Accepted Manuscript or any consequences arising from the use of any information it contains.

Evaluating the merit of a diethylamino coumarin-derived thiosemicarbazone as an intramolecular charge transfer probe: efficient Zn (II) mediated green to yellow emission swing

Arghyadeep Bhattacharyya, Subhash Chandra Makhil, and Nikhil Guchhait*

Department of Chemistry, University of Calcutta, 92, A.P.C. Road, Kolkata-700009, India

*Corresponding author. Tel.: +913323508386; fax: +913323519755.

E-mail address: nguchhait@yahoo.com (N. Guchhait).

Abstract: We report the synthesis and photophysical properties of a coumarin based probe (1E)-1-(1-(7-(diethylamino)-2-oxo-2H-chromen-3-yl) ethylidene) thiosemicarbazide (**DIDOT**). **DIDOT** shows polarity dependant change on the emission maxima in solution phase. This is explained by the considering increased dipole moment in the excited state by intramolecular charge transfer (**ICT**) process. **DIDOT** can successfully detect Zn (II) in aqueous methanol by shifting of its charge transfer emission maxima from ~506 nm to ~535 nm. The shifting could be conceived by change in color from green to yellow under UV-light. The mechanism of Zn (II) detection has been delineated by ESI-MS, FTIR and fluorescence time resolved studies coupled with theoretical calculations. Increment in charge transfer in the Zn (II) complex of **DIDOT** over the bare receptor as a consequence of conformational locking was attributed to be the underlying cause of the cation detection phenomenon. The limit of detection and binding constant values of **DIDOT** towards Zn (II) are respectively $\sim 3 \times 10^{-8}$ M and 2.35×10^5 M⁻¹ respectively. Finally, the practical utility of **DIDOT** has been demonstrated by successful detection and quantification of Zn (II) in spiked water samples.

Introduction

The selective and sensitive detection of Zn in its dipositive form is a relevant area of research. The relevance arises due to the effect Zn (II) exerts on the human body as well as on environment. Being the second most abundant element in the human body¹, Zn (II) is of utmost importance as far as cell division², clotting of blood³, repairmen of DNA⁴ and protein synthesis⁵ processes are concerned. However, an excess accumulation of the same within the body adversely affects hair growth⁶, brain functioning⁷ and blood cholesterol level⁸. Zinc is also reported to be involved in causing neurodegenerative diseases like Alzheimer's⁹. Leaching of Zn (II) in water makes it smelly and muddy, whereas Elevated levels of Zn in soil inhibit microbial activity, thereby exerting phytotoxic effects¹⁰. WHO has thus recommended limit for Zn (II) in water to be 76 μM ¹¹. Hence, selective and sensitive detection of Zn (II) dissolved in water along with proper quantification by synthesized chemosensors thus remains a challenge. While detecting Zn (II), the fluorimetric¹² as well as colorimetric¹³ mode of detection are widely practiced due to the cost effective and easy handling of instruments. The challenge arises mainly due to competition with other similar sized cation Cd (II) ¹⁴⁻¹⁷, which offers similar spectral response to Zn (II) as was reported previously by various groups. Although there are large numbers of reports of selective chemosensors for Zn (II), the mode of response in such reports deals with the variation of the emission intensity of the receptors, a phenomenon which can also be affected by surrounding environment due to the sensitive nature of emission spectroscopy¹⁸. For this purpose, probes which show a shifting in their emission maxima would be more accurate for the detection for Zn (II). Previously, we reported a coumarin based probe which underwent a 44 nm red shifting of its emission maxima in presence of Zn (II) ¹⁹. The current report is an advanced modification to our previous reports, in which we synthesized thiosemicarbazone of 7-

diethylamino 3-ethylcoumarin, named (1E)-1-(1-(7-(diethylamino)-2-oxo-2H-chromen-3-yl) ethylidene) thiosemicarbazide (**DIDOT**) for the detection of Zn (II) ion. The choice of 7-diethylamino coumarin was principally due to strong emissive nature of its derivatives²⁰. Thiosemicarbazide was chosen due to the affinity of the said molecule and its derivatives towards Zn (II)²¹. **DIDOT** was previously utilized as an intermediate in the synthesis of some antibacterial agents by Yuan et al²². However, its spectroscopic characterization as well as sensing aptitude had not been explored prior to the current report. Due to presence of hard donor atoms in the form of N as well as O enabled **DIDOT** to be a Zn (II) specific probe^{13, 19}. **DIDOT** shows excellent solvatochromic shift in its emission profile depending on solvent polarity and can detect Zn (II) by a remarkable shift in its emission maxima from ~506 nm to ~535 nm upto a lowest detection limit of $\sim 3 \times 10^{-9}$ M. Most importantly, this shifting in emission maxima was evident when observed under UV-light, where the solution of **DIDOT** turns yellow from green in presence of Zn (II). This increases the efficacy of **DIDOT** over other available Zn-selective probes as the change in color under UV-light enables one to detect Zn (II) easily by observing yellow coloration. Furthermore, by utilizing **DIDOT** as a Zn (II) specific probe, we have improved our own previous report¹⁹ as the previous report afforded turn on detection whereas the current one causes emission swing from green to yellow in presence of Zn (II). The binding nature and mechanism of Zn (II) detection were well established by ESI-MS, Job's plot analysis, Benesi-Hildebrand (B-H) plot and time-resolved emission studies. Zn (II) detection by **DIDOT** was applied by successful detection and quantification of the cation in spiked water sample. Thus, green to yellow emission switching in presence of Zn (II) along with the low detection limit towards the aforesaid metal ion makes **DIDOT** a lucrative receptor for detection of Zn (II).

Furthermore, the interesting excited state solvatochromism of **DIDOT** makes it a potential fluorescent probe for future applications.

Experimental

Chemicals

4-diethylamino salicylaldehyde, ethyl acetoacetate, thiosemicarbazide, perchlorate salts of cations, sodium salts of anions were purchased from Sigma Aldrich and used as received. All spectroscopic studies were performed using spectroscopic grade solvents from Spectrochem. Triple distilled water was used for preparation of the solutions of cations and anions.

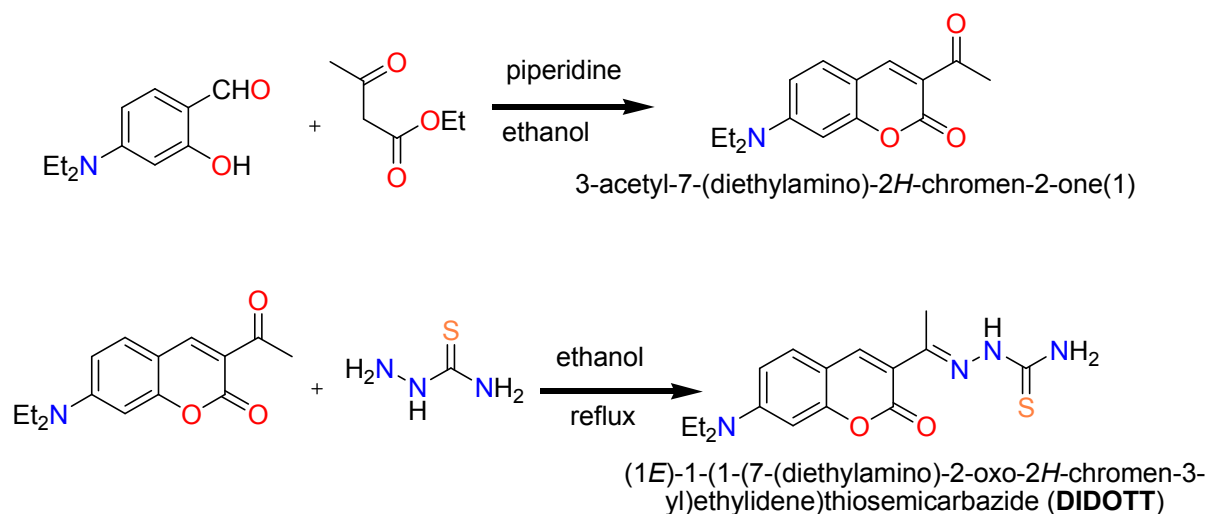
Syntheses

Synthesis of **DIDOT**

The synthesis of **DIDOT** was achieved by two simple steps (Scheme 1) as discussed below.

Step I. Synthesis of 7-diethylamino 3-acetyl coumarin (1)

4-diethylamino salicylaldehyde (1.93 g, 10 mmol) was dissolved in 20 mL ethanol, followed by addition of equimolar amount of ethyl acetoacetate. 10 mmol of piperidine was added to the reaction mixture while being stirred at room temperature. After stirring overnight, bright yellow crystalline solid separated from the reaction mixture. It was filtered under suction, washed with 50% aqueous ethanol and dried in open air. The yield was 90%. ^1H NMR and ^{13}C NMR spectra were recorded in CDCl_3 for the purpose of characterization. ^1H –NMR (ESI, Fig. S1) (300 MHz, CDCl_3 , 290 K, TMS): 8.35(s, 1H), 7.30(d, 1H), 6.53-6.57 (m, 1H), 6.39(d, 1H), 3.419-3.348(q, 4H), 2.598(s, 3H) and 1.142-1.190(t, 6H). ^{13}C NMR (ESI, Fig. S2) (75 MHz, CDCl_3 , 290 K, TMS): 195.6, 160.8, 158.7, 152.9, 147.7, 131.8, 116.2, 109.9, 108.2, 96.7, 45.0, 30.5 and 12.4.



Scheme 1. Synthesis of (1*E*)-1-(1-(7-(diethylamino)-2-oxo-2*H*-chromen-3-yl) ethylidene) thiosemicarbazide (DIDOT)

1 (2.0 mmol) was dissolved in ethanol by continuously stirring **1** at 80° C in a 50 mL round bottom flask. Then solid thiosemicarbazide (0.2 g) was added to the hot ethanolic solution of **1** in ethanol, followed by addition of 50 μ L of acetic acid. The reaction mixture was refluxed with stirring overnight, resulting in separation of a brick red powder. It was filtered under suction, washed with 50% aqueous ethanol several times to remove traces of thiosemicarbazide, if any and finally dried at 80° C for 6 hours. **DIDOT** was obtained in 65% yield as fine brick red powder. It was characterized by FTIR (ESI, Fig. S3), ¹HNMR (ESI Fig. S4), ¹³C NMR (ESI, Fig. S5) and ESI-MS (ESI, Fig. S6). FTIR (KBr, cm⁻¹): 3404, 3243, 2971, 1715, 1618, 1595, 1567, 1508 and 1230. ¹H -NMR (300 MHz, DMSO-d₆, 290 K, TMS): 10.25 (s, 1H), 8.29-8.32 (d, 2H), 7.86 (s, 1H), 7.45-7.48 (s, 1H), 6.71-6.75 (m, 1H), 6.53 (s, 1H), 3.4-3.47 (q, 4H), 2.22 (s, 3H), 1.09-1.14 (t, 6H). ¹³C -NMR (75 MHz, DMSO-d₆, 290 K, TMS): 179.3, 160.4, 156.9, 151.5, 147.7, 143.2, 130.7, 117.8, 109.9, 108.3, 96.5, 44.6, 16.5, 12.8. ESI-MS: molecular formula for [M-H]⁺ C₁₆H₂₁N₄O₂S, calculated m/z value, 333.1385, obtained 333.1367.

Synthesis of DIDOT-Zn (II) complex

DIDOT (0.5 mmol) was suspended in 10 mL ethanol and 1.0 mmol of Zinc perchlorate hexahydrate dissolved in 2 mL water was added drop wise, resulting in a clear dark red solution. Overnight stirring at room temperature furnished a dark red powder. It was confirmed to be the Zn complex of **DIDOT** by FTIR (ESI, Fig. S7) and ESI-MS (ESI, Fig. S8). FTIR (KBr, cm^{-1}): 3433, 2924, 1620, 1574, 1510, 1420, 1345, 1109, 1086, 805, 626. ESI-MS: calculated 413.0626, obtained 413.2697.

Instruments

^1H -NMR and ^{13}C -NMR were recorded on Bruker Advanced Supercon 300 MHz and chemical shifts are expressed in ppm using TMS as internal standard. FTIR spectrum was recorded on Perkin Elmer spectrum-100 and UV-Vis experiments were conducted in Hitachi U-3501 Spectrophotometer. Mass spectrometry was carried out in Waters Xevo G2-S Q TOF. Fluorescence titration and excited state lifetime measurements using Time Correlated Single Photon Counting (TCSPC) method were carried on in Perkin Elmer LS-55 and Horiba Jobin Yvon Fluorocube-01-NL respectively.

Theoretical Calculations

DIDOT as well as its Zn (II) complex was optimized using Gaussian 09W using B3LYP hybrid functional (6-311++g** basis set)²³. The structures were manually constructed with the aid of Gauss view prior to optimization.

Results and discussions

Photophysical properties of DIDOT

The photophysical properties of **DIDOT** were investigated in solution phase in various solvents. All measurements were carried out using micro molar solutions of **DIDOT** to avoid reabsorption effect in the absorption spectroscopy and self-quenching in the emission spectroscopic studies. The absorption profiles of **DIDOT** in various solvents (Fig. 1) showed a single absorption band ranging from 400-450 depending on the polarity of the solvents (Table 1). In non-polar medium like heptane, a sharp absorption band was obtained at 410 nm. However, in water, a broad band centered at around 450 nm was obtained. The red shift in the absorption maxima with solvent polarity could be due to different extent of stabilization of the excited state compared to the ground state²⁴. The single absorption band is assigned to be due to π - π^* transition by accounting for the polarity dependence of the said band²⁵. The emission profiles in various solvents were recorded by exciting **DIDOT** at ~410 nm (Fig. 1). In non-polar solvent heptane the emission profile was broad in nature with maxima around 450 nm. The maximum was further shifted in chloroform and attained a value of ~475 nm. This red shifting was observed as more polar solvents were observed and in water, the emission band was centered on 515 nm. In butanol, the emission maxima underwent blue shifting compared to methanol and water. This may be due to the cumulative effect of H-bonding and viscosity of the solvent in question. Interestingly, a blue sided shoulder emission band was observed over the red shifted emission maxima in solvents like acetone, acetonitrile and DMSO. As polarity dependant shift in emission maxima indicated the greater dipolar character of the excited state in **DIDOT**, a higher value of the excited state dipole moment is expected for the probe in question. To verify this assumption, we constructed Lippert plot as well as Lippert-Mataga plots²⁶ to find out the ground and excited state dipole

moments (Fig. 2) of **DIDOT**. In both cases reasonable linearity was obtained. This was assured by plotting the Stokes' Shift ($\nu_a - \nu_e$) values of **DIDOT** in various solvents. The Onsager cavity radius required for the calculation of the dipole moments was found out to be 5.81 Å from theoretical volume calculation of **DIDOT** for the ground state optimized geometry (DFT calculation with B3LYP hybrid functional and 6-311++g** basis set). The calculated values of ground and excited states were 3.2 D and 6.8 D respectively. Furthermore, a plot of the emission maxima values against the $E_T(30)$ values of solvents furnished two slopes according to the proticity of the solvents, suggesting both dipolar as well as hydrogen bonding interactions are prevalent with the solvent(s) in the excited state of **DIDOT** (Fig. 3a)²⁷. A reasonable linear relation was obtained between the emission wave number ν_e and the solvent hydrogen bonding parameter (α) (Fig.3b)²⁸. The enhanced value of the excited state dipole moment along with the previously discussed results suggested that the excited state photophysical properties of **DIDOT** may be guided by relatively higher excited state dipole moment which may possible through intramolecular charge transfer (ICT) from diethylamino moiety to the imine moiety of the molecule (ICT) (Scheme 2). The fluorescence excitation spectra were recorded (ESI, Fig. S9) and resembled the absorption profiles of **DIDOT** in various solvents. Interestingly, the excitation spectra for the shoulder band and the maxima furnished a single band, suggesting both the bands were furnished by excitation from the same electronic state^{29, 30}. The quantum yields of **DIDOT** in solvents were also calculated (Table 1). Interestingly, the quantum yield values increased somewhat steadily till DMSO and experienced a decrement in protic solvents. This could be rationalized owing to the stabilization of the excited state charge transfer in polar aprotic solvents, whereas deexcitation triggered by Hydrogen bonding interactions in polar protic solvents could account for the aforementioned observation³¹.

Table1. Spectral Information of DIDOT in various solvents (solvent abbreviation provided in ESI)

Solvent	$\lambda_{\text{max}}^{\text{abs}}(\text{nm})$	$\lambda_{\text{max}}^{\text{em}}(\text{nm})$	Fluorescence Quantum Yield (Φ_f)
Hep	399	449	0.020
Cy	402	453	0.030
CHCl ₃	418	475	0.040
DCM	416	483	0.021
Acetone	411	475, 502	0.010
ACN	415	475, 509	0.052
DMSO	423	475, 512	0.090
MeOH	422	506	0.065
n-BuOH	430	475, 492	0.035
Water	440	515	0.011

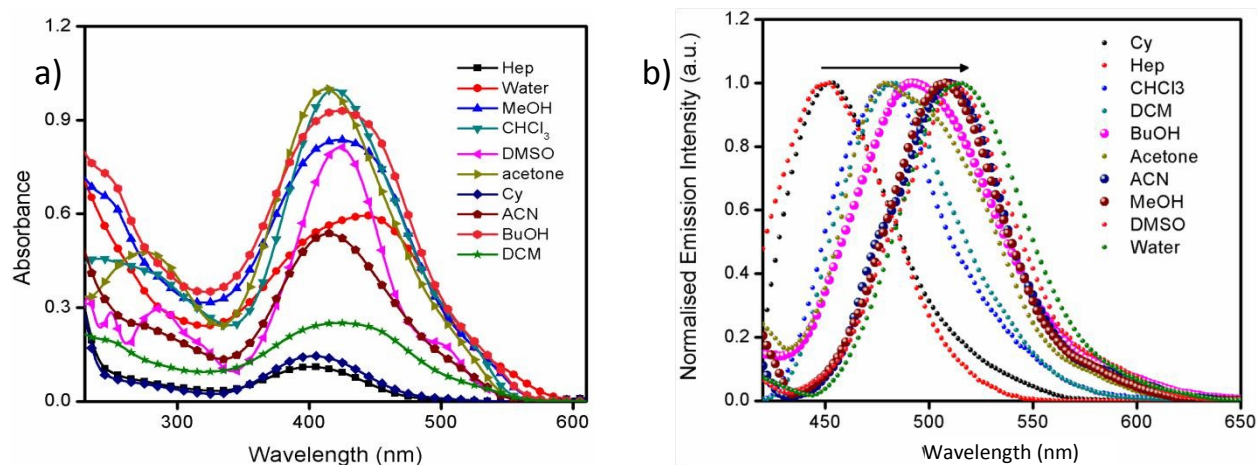


Figure 1: (a) Absorption profiles of **DIDOT** in various solvents. (b) Normalized Emission profiles of **DIDOT** in various solvents ($\lambda_{\text{ex}}=410$ nm).

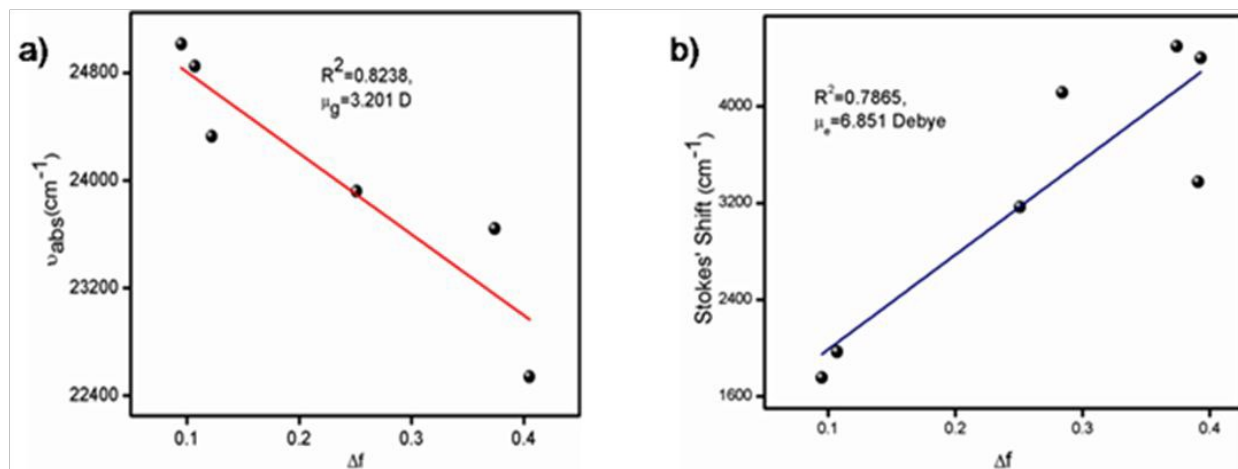


Figure 2: (a) Lippert plot. (b) Lippert-Mataga plot.

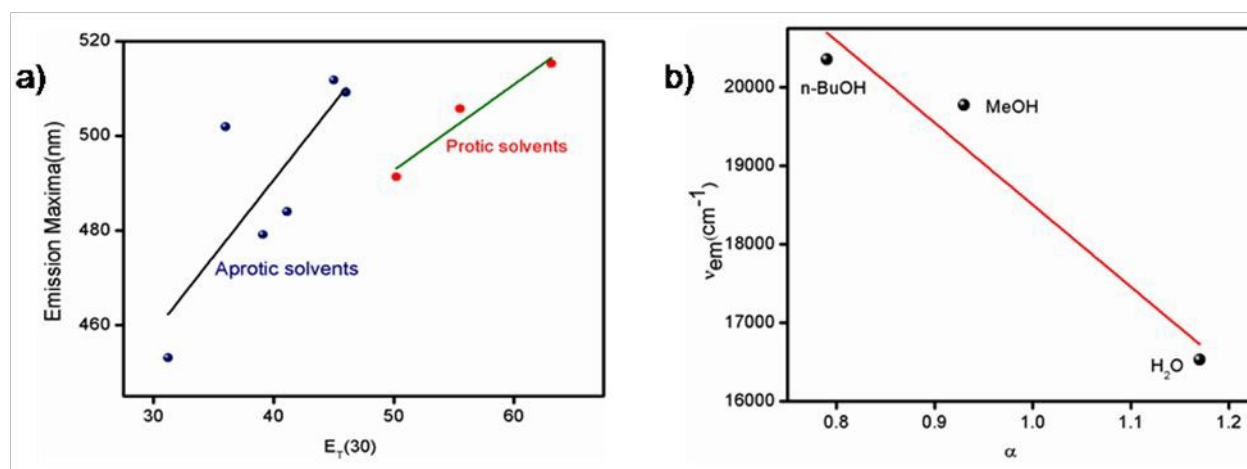
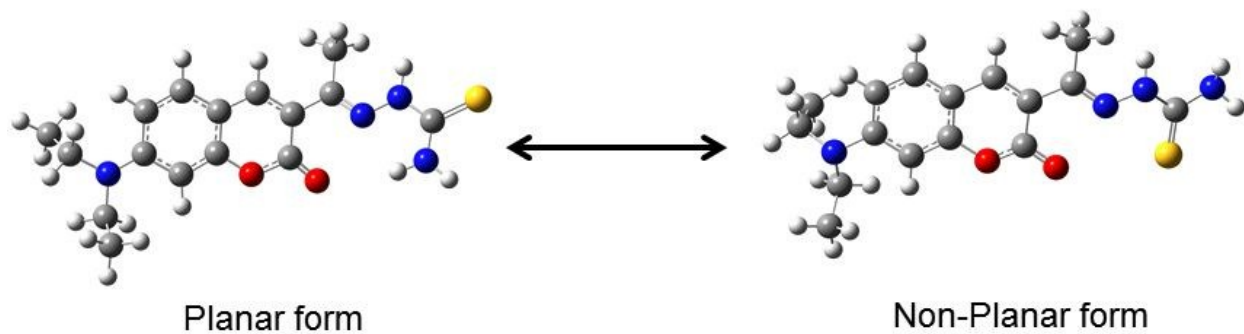


Figure 3: (a) Plot of emission maxima against $E_T(30)$ parameter. (b) Plot of emission wave number values against Hydrogen bonding parameter of solvents.

Excited State Lifetime measurements

To probe the excited state dynamics of **DIDOT**, TCSPC experiments were conducted. The decay profiles obtained were deconvoluted using DAS-6 software and the goodness of fit was based on χ^2 criteria. The relative population of excited state species and average lifetime values were calculated using standard protocol³¹. **DIDOT** was excited using a 375 nm LASER diode and the decays were monitored at the corresponding emission maxima according to the solvent. **DIDOT** showed a bi-exponential decay irrespective of the nature of the solvent (Fig. 4, Table 2). There existed a component having lifetime in the order of picoseconds, whereas a slower component having lifetime in the order of nanoseconds was recorded. In case of polar solvents the emission decay was calculated to have faster lifetime with larger amplitude (Table 2). In non-polar solvents like heptane and cyclohexane, the slow component shows larger amplitude. Since thiosemicarbazone bearing probes are often used as chemosensors for metal ions, we consequently checked the response of **DIDOT** towards metal ions.



Scheme 2: Calculated optimized planar and non-planar forms of **DIDOT** (DFT level with B3LYP hybrid functional and 6-311++g** basis set).

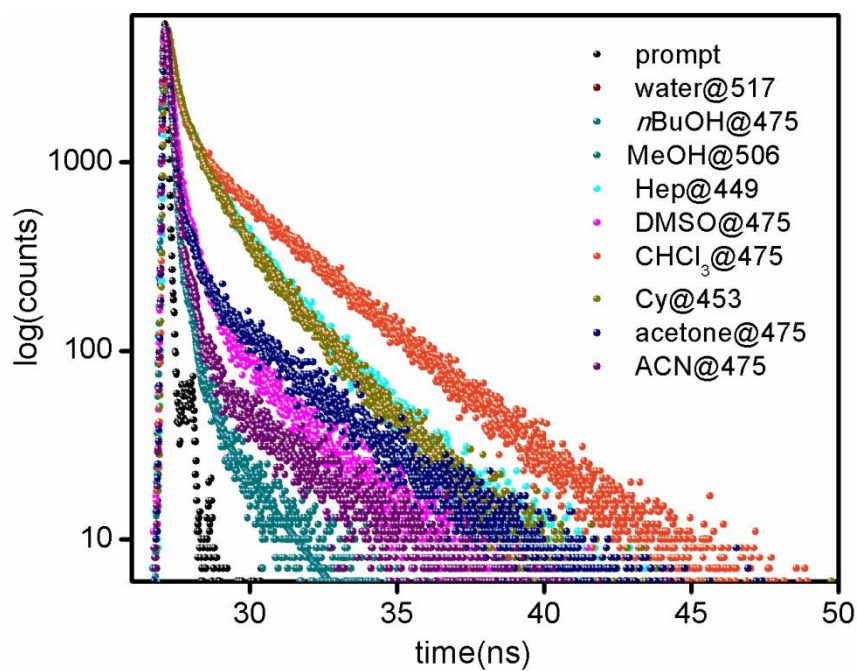


Figure 4: Decay profiles of **DIDOT** in various solvents ($\lambda_{\text{ex}}=375$ nm).

Table 2. Excited state decay parameters of **DIDOT** in various solvents

Solvent(λ_{mon})	$\tau_1(\text{s})/B_1$	$\tau_2(\text{s})/B_2$	$\tau_{\text{av}}(\text{ps})$	χ^2
Hep (449)	$3.98 \times 10^{-10}/35$	$2.21 \times 10^{-9}/65$	851	1.23
Cy (453)	$4.35 \times 10^{-10}/40$	$2.25 \times 10^{-9}/60$	844	1.18
CHCl ₃ (475)	$3.34 \times 10^{-10}/27$	$3.15 \times 10^{-9}/73$	972	1.20
ACN (475)	$2.00 \times 10^{-10}/80$	$2.73 \times 10^{-9}/20$	173	1.30
ACN (510)	$1.63 \times 10^{-10}/95$	$3.04 \times 10^{-9}/5$	173	1.12
DMSO (475)	$2.66 \times 10^{-10}/70$	$2.49 \times 10^{-9}/30$	362	1.08
DMSO (512)	$2.77 \times 10^{-10}/90$	$2.91 \times 10^{-9}/10$	304	1.13
MeOH (506)	$1.45 \times 10^{-10}/91$	$1.86 \times 10^{-9}/9$	159	1.15
<i>n</i> -BuOH (475)	$4.93 \times 10^{-10}/77$	$4.75 \times 10^{-9}/23$	625	1.00
<i>n</i> -BuOH (492)	$4.39 \times 10^{-10}/87$	$4.21 \times 10^{-9}/13$	498	
Water (515)	$4.19 \times 10^{-10}/96$	$3.58 \times 10^{-9}/4$	435	0.94

Cation recognition by DIDOT

The response of **DIDOT** towards metals was initially checked by observing the naked eye color change of a 50 μM methanolic solution of **DIDOT** after separately adding 10 equivalents of metal perchlorate salt. The yellow color of **DIDOT** solution turned reddish in presence of Cu (II), yellowish in presence of nickel (II) and cadmium (II) and there was a deepening in color in presence of almost all other metal ions (Fig. 5). Thus, no selectivity was assured from naked eye

color change. Then the changes in absorption profile of **DIDOT** were checked in presence of metals.

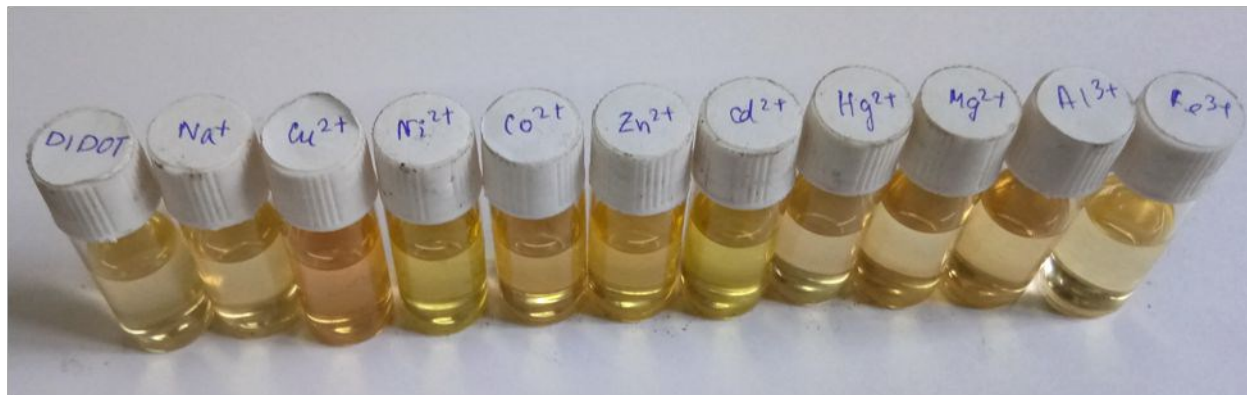


Figure 5: Change in color of a 50 μM methanolic solution of **DIDOT** in presence of 10 equivalents of various metal ions observed under ambient light.

Addition of all metal ions (2 equivalents) to **DIDOT** (10 μM) perturbed the absorption profile of the latter (ESI, Fig. S10). Thus, no selectivity could be ensured for any metals from the naked eye color change as well as UV-Visible experiments. Finally, we checked whether there is any selectivity as far as the fluorogenic response is concerned. For this purpose, color of solutions containing **DIDOT** as well as mixture of **DIDOT** and metal salts were checked under UV-light first. Interestingly, **DIDOT** itself shows a prominent green color under UV-light. However, addition of only Zn (II) afforded a change in color from green to bright yellow. Addition of other metals did not cause any such change in color as Zn (II) (Fig. 6). The emission profile of **DIDOT** also experienced a red shift in accordance to naked eye color change under UV light in presence of Zn (II) (Fig. 7).

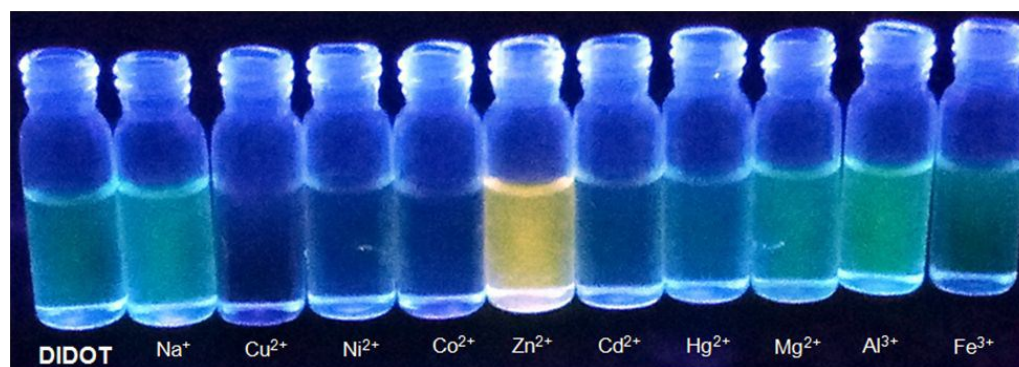


Figure 6: Change in color of a 50 μM methanolic solution of **DIDOT** in presence of 10 equivalents of various metal ions observed under UV-light.

The emission maxima of a 5 μM methanolic solution of **DIDOT** undergoes a red shift from ~ 506 nm to ~ 535 nm upon addition of 2 equivalents of Zn (II). Addition of other metal ions afforded simple quenching or no change in the emission profile of the probe. An emission titration was conducted by addition of Zn (II) to **DIDOT** where the new band at ~ 534 nm increased in intensity upon gradual addition of the metal ion. Presence of an isoemissive point at ~ 480 nm ensured the presence of equilibrium between **DIDOT** and its Zn (II) complex. Using standard protocol³² the limit of detection was calculated using the equation, $\text{LOD} = \frac{3\sigma}{\text{Slope}}$, where σ is the standard deviation and slope is that of the calibration curve. The limit of detection towards Zn (II) was calculated to be in the order of $\sim 3 \times 10^{-8}$ (M) (ESI, Fig. S11). The low limit of detection well establishes the efficacy of **DIDOT** when compared to the limits of detection of previously reported Zn (II) specific probes (ESI, Table S1).

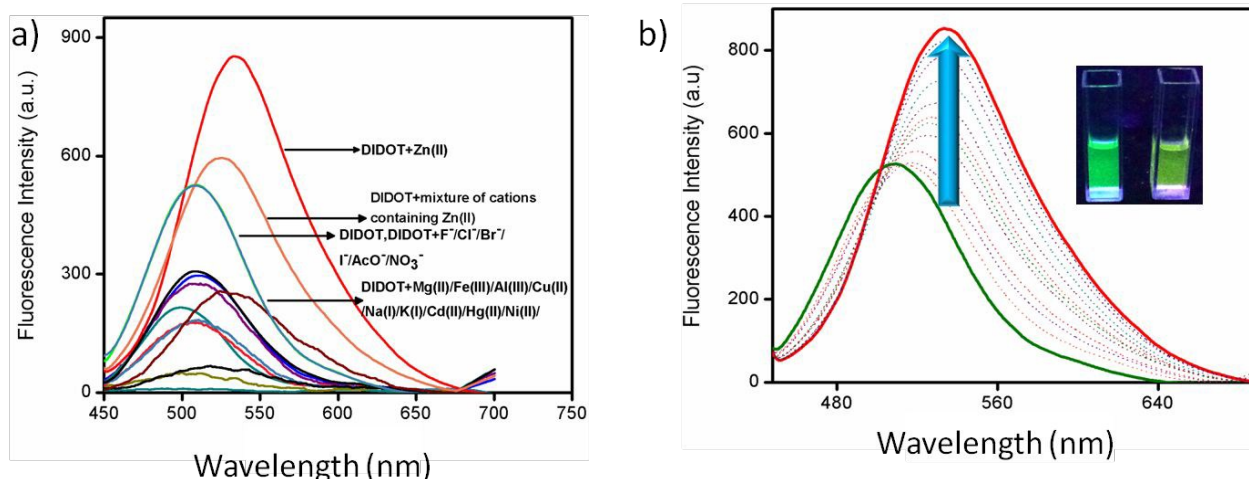


Figure 7: (a) Emission profiles of **DIDOT** and **DIDOT**+ various metal ions ($\lambda_{\text{ex}}=410$ nm). (b) Emission titration of 5 μM solution of **DIDOT** with 0- 2 equivalents Zn (II); (inset) change in color of solution of **DIDOT** after Zn (II) titration as observed under UV-light.

Binding nature of **DIDOT** with Zn (II)

The binding pattern of **DIDOT** with Zn (II) was first explored by Job's plot analysis³³, where a 1:1 binding pattern of the two species (Fig. 8). The binding constant value was calculated by constructing B-H plot³⁴ assuming 1:1 stoichiometry of binding using the emission titration data (Fig. 8). An excellent linear fit was obtained and the binding constant value was thus calculated to be $2.355 \times 10^5 \text{ M}^{-1}$. Such a high binding constant value accounts for the affinity of **DIDOT** towards Zn (II). Further evidence of 1:1 complexation was obtained upon recording the ESI-MS of **DIDOT**-Zn complex where a mass corresponding to 1:1 complex formation was observed (Fig. S8). While analyzing the results of mass spectrometric analysis, the observed mass could be explained only by assuming the deprotonation of the amine proton in **DIDOT** while undergoing complexation with Zn (II). Presence of a water molecule as observed from the mass spectrum completes the co- ordination sphere of the Zn (II) ion undergoing complexation. This was

supported by FTIR analyses. If the FTIR spectra of **DIDOT** and its Zn (II) complexes are compared, the sharp signal for $-\text{NH}_2$ group in **DIDOT** is changed to a broad signal in the complex. Furthermore, the shift in the values of imine signal (1715 cm^{-1} in free **DIDOT** to 1620 cm^{-1} in Zn (II) complex) indicates the involvement of the aforesaid moiety in the complexation process. The involvement of coumarin nucleus is also expected as a change in the emission maxima of **DIDOT** in presence of Zn (II). The only possible mode of binding of coumarin moiety with Zn (II) is by means of forming a co-ordinate covalent bond between the ester carbonyl moiety of **DIDOT** and Zn (II). From all the above observations, it was concluded that **DIDOT** forms a 1:1 complex with Zn (II) forming 6 member and 5 member chelate rings (Scheme 3). However, coordination through Sulfur centre could not be possible as i) the soft Sulfur donor and hard Zn (II) ion would not form a very stable bond. ii) For a chelate ring bearing an endocyclic double bond, a six member ring would be thermodynamically favoured over a 5- member ring³⁵.

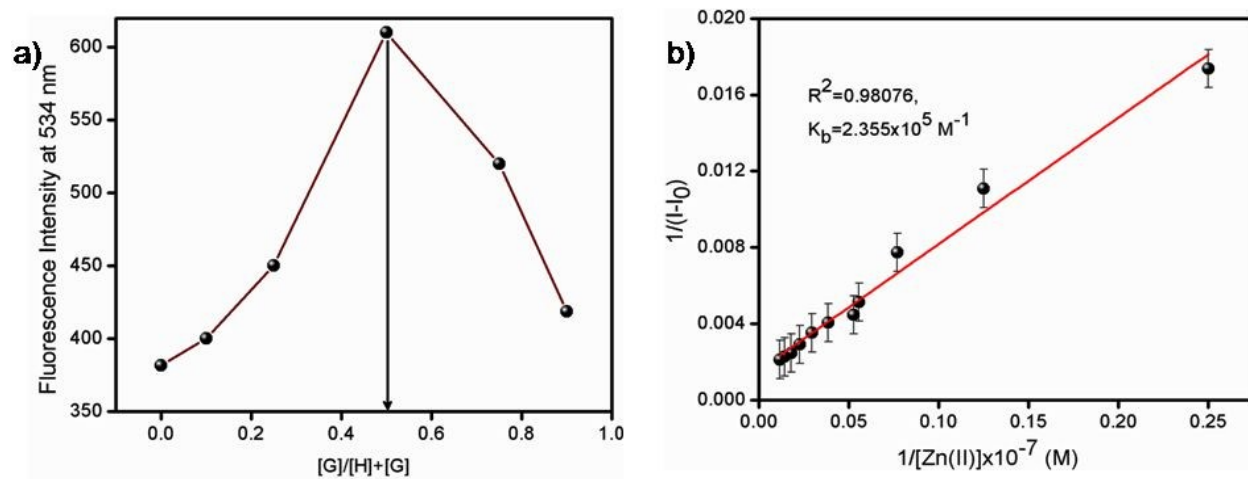


Figure 8: a) Job's plot and b) B-H plot for **DIDOT** and Zn (II).

Mechanism of Zn (II) detection

To probe the mechanistic pathway of Zn (II) detection by **DIDOT**, TCSPC experiments were conducted. As can be seen from Table 2, bare **DIDOT** showed an average lifetime of 159 ps. Upon addition of 1 equivalent of Zn (II), the average lifetime was calculated to be 1727ps (Fig. 9, Table 3). Apart from increment in the lifetime, the faster lifetime component ($\tau \sim 145$ ps) in **DIDOT** underwent a considerable increment to attain a value of ~ 1590 ps in presence of Zn (II) whereas the component having higher lifetime value ($\tau \sim 1860$ ps) showed lifetime in the same order in presence of Zn (II) ($\tau \sim 3700$ ps). Thus, from our earlier assignment of lifetime components of **DIDOT**, the planar form of the same experiences enhancement in the lifetime upon complexation with Zn (II). This could be justified based on the attainment of rigidity in the flexible structure of **DIDOT** post complexation, as encountered often in case of Chelation Induced Enhancement of Fluorescence (**CHEF**) mechanism³⁶⁻³⁷. To verify this, the emission profile of **DIDOT** in polyethylene glycol-400 (PEG400), a viscous solvent, was recorded (Fig.10a). However, the emission profile of **DIDOT** in PEG400 exhibited in only enhancement of the fluorescence intensity, without any noticeable shift in the emission intensity. Thus, the attainment in rigidity of **DIDOT** upon complexation only accounted for emission intensity enhancement. But the shift in emission maxima was yet to be explained. Since **DIDOT** contains a diethyl amino group as a donor and a keto imine as an acceptor, there is charge transfer from the former to the latter, owing to the electron withdrawing character of the imine group. However, electron donation from the thiosemicarbazone linkage adjacent to the imine moiety partially quenches the **ICT** in **DIDOT**, reflected by the small increment in the excited state dipole moment value of **DIDOT** (Scheme 3). However, the engagement of the imine as well as the thiosemicarbazone moieties along with the coumarin nucleus in complexation process with

Zn (II) is expected to facilitate the charge transfer from the diethylamino moiety to the imine moiety (Scheme 3). This assumption was verified by recording the emission profiles of **DIDOT**-Zn complex in acetonitrile and methanol (Fig. 10b). The results showed that the emission profile in acetonitrile was ~525 nm, whereas the same in methanol was ~534 nm. This shift in emission maxima was consistent keeping in mind the $E_T(30)$ values of the two solvents (~46.0 for acetonitrile and ~56 for methanol). Thus, the shift in emission maxima of **DIDOT** after complexation with Zn (II) is a consequence of increased charge transfer from diethylamino moiety to the imine moiety. This was also supported from considering the Mulliken charge densities of **DIDOT** and its Zn (II) complex, explained in details in the subsequent theoretical calculation section. The increment in lifetime of **DIDOT**-Zn (II) ensemble is due to the rigid structure of the same, which results in freezing of non-radiative decay channels in the said species. Thus, **DIDOT** detects Zn (II) by arresting of the conformation in presence of Zn (II) followed by enhanced ICT from diethylamino moiety to the imine carbon. The fluorescence intensity enhancement is due to CHEF operative in the rigid structure of the **DIDOT**-Zn complex.

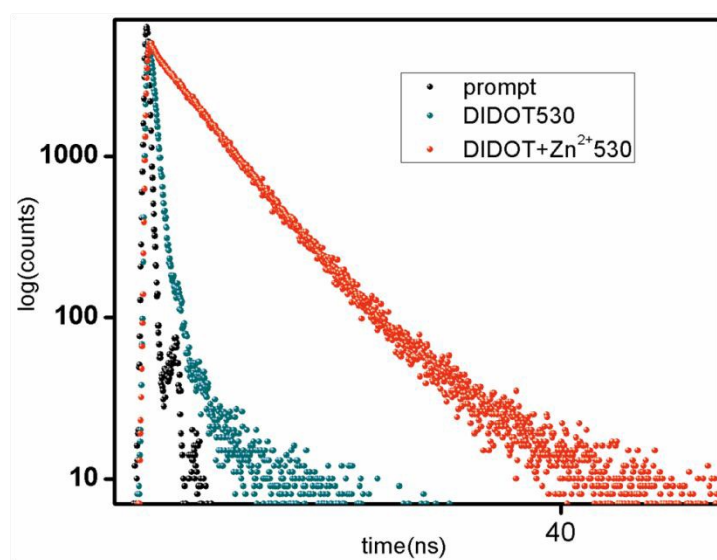


Figure 10: (a) Comparative emission profiles of **DIDOT** in MeOH and PEG400, (b) Comparative emission profiles of **DIDOT-Zn** complex in ACN and MeOH.

Table 3. Excited state decay parameters of **DIDOT-Zn** in MeOH ($\lambda_{\text{mon}}=530$ nm)

Species	$\tau_1(\text{ps})/B_1$	$\tau_2(\text{ps})/B_2$	$\tau_{\text{av}}(\text{ps})$	χ^2
DIDOT	182/91	1940/9	198	1.20
DIDOT-Zn	1590/87	3810/13	1727	1.09

Theoretical calculations

DIDOT (ESI, Fig.S12) and its Zn (II) complex were optimized and the important structural parameters are provided in Table S2 of ESI. Two conformers were optimized for **DIDOT** and designated as planar form (**P**) and non-planar form (**NP**) respectively (Scheme 2). The designation has been done considering the dihedral angle (Θ_d) values of the two conformers about the imine-thiosemicarbazone linkage. In **P** form, the Θ_d value is 25° whereas the same in **NP** form is 38° . The free inter conversion between the two conformers as proposed earlier is justified from calculating the energy gap ($\Delta E_{\text{HOMO-LUMO}}$) between the Highest Occupied Molecular Orbital (HOMO) and Lowest Unoccupied Molecular Orbital (LUMO) for each receptor (ESI, Fig. S13). The energy gap is comparable in both conformers, allowing conversion between the two. The charge density analyses on the two conformers (ESI, Table S3) show that for **P** form and **NP** form, the Mulliken charges on the carbon adjacent to the imine moiety are -0.168 and -0.145 respectively (Table S3). However, in case of the Zn (II) complex, from all the experimental results, **P** form was concluded to undergo complexation with the metal. In the

complex, the charge on the same carbon attained a value of +0.075 (Table S2, Fig. S13), which supports our proposal that greater charge transfer, occurs from diethylamino group to the imine group in **DIDOT** post complexation with Zn (II). The dihedral angle value of the complex (22°) indicates that the complex bears structural resemblance to the **P form**. Hence, charge transfer is expected to be enhanced in **DIDOT** post complexation with Zn (II). The stability attained by the Zn (II) complex of **DIDOT** is supported from decreased HOMO-LUMO gap compared to either conformers of **DIDOT** (ESI, Fig. S14). Hence, the theoretical calculations aid in understanding the photophysical modulation of **DIDOT** upon complexation with Zn (II).

Practical application of **DIDOT**

In spite of the remarkable photophysical modulation of **DIDOT** in presence of Zn (II), the main bottleneck in using it for practical purposes was the use of methanol as the sensing medium. To overcome this limitation, an alternative approach was considered. Two 10 mL spiked water samples containing Zn (II) were prepared with varying concentrations of Zn (II) in them. An aliquot of 50 μL was added from both the samples to the methanolic solution of **DIDOT**. The emission profiles were recorded, each point being recorded as triplicate. **DIDOT** was able to detect the Zn (II) in both water samples (Fig. 11) and the results are provided in Table S4 of ESI. In both the cases, the relative error was well below 10%, ensuring accuracy of measurement. Hence, the fluorogenic detection and quantification of Zinc in water samples was achieved by **DIDOT**.

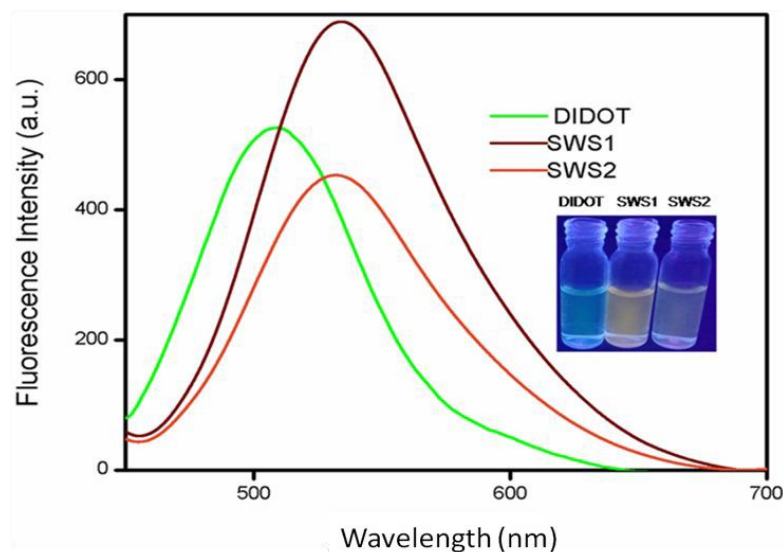


Figure 11: Emission response of **DIDOT** towards two spiked water samples labeled **SWS1** and **SWS2**.

Conclusion

In conclusion, the current work involves Zn (II) detection by interesting modulation of the excited state photophysics of a coumarin based ICT compound **DIDOT**. The photophysical characterization of **DIDOT** has been conducted thoroughly along with proper explanation of the Zn (II) detection mechanism by theoretical and experimental methods. The limit of detection of **DIDOT** towards Zn (II) is ~30 nM. **DIDOT** can successfully detect and quantify water in drinking water sample.

Conflict of interest

There are no conflicts of interest.

Acknowledgement

A.B and S.C.M gratefully acknowledge senior research fellowships from CSIR and UGC, New Delhi, Government of India, respectively. NG likes to acknowledge DST, India (Project No. EMR/2016/004788) for financial support.

References

1. E. L. Que, D. W. Domaille and C. J. Chang, Metals in neurobiology: probing their chemistry and biology with molecular imaging, *Chem. Rev.*, 2008, **108**, 1517–1549.
2. Q. Lin, Y. Cai, Q. Li, J. Chang, H. Yao, Y. M. Zhang and T. B. Wei, A simple pincer-type chemosensor for reversible fluorescence turn-on detection of zinc ion at physiological pH range, *New J. Chem.*, 2015, **39**, 4162-4167.
3. D. Sarkar, A. K. Pramanik and T. K. Mondal, A novel coumarin based molecular switch for dual sensing of Zn (II) and Cu (II), *RSC Adv.*, 2015, **5**, 7647-7653.
4. S. Mandal, Y. Sikdar, D. K. Maiti, G. P. Maiti, S. K. Mandal, J. K. Biswas and S. Goswami, A new pyridoxal based fluorescence chemo-sensor for detection of Zn (II) and its application in bio imaging, *RSC Adv.*, 2015, **5**, 72659-72669.
5. J. H. Kim, J. Y. Noh, I. H. Hwang, J. Kang, J. Kim and C. Kim, A NBD-based selective colorimetric and fluorescent chemosensor for Hg²⁺, *Tetrahedron Lett.*, 2013, **54**, 2415-2418.
6. D. L. Ma, L. Wang, H. Z. He, M. Y. S. Lee, H. J. Zhong, S. Lin, C. H. Leung, S. H. D. Chan and C. Y. Wong, *ACS Appl. Mater. Interfaces*, 2014, **6**, 14008-14015.

7. A. Ghosh, S. Ta, T. K. Dangar, M. Ghosh, S. K. Mukhopadhyay, S. Karmakar, A. Banik and D. Das, Dual mode ratiometric recognition of zinc acetate: nanomolar detection with in vitro tracking of endophytic bacteria in rice root tissue, *Dalton Trans.*, 2016, 45, 599-606.
8. Z. Guo, G. H. Kim, I. Shin and J. Yoon, A cyanine-based fluorescent sensor for detecting endogenous zinc ions in live cells and organisms, *Biomaterials*, 2012, **33**, 7818-7827.
9. A. I. Bush, The metallobiology of Alzheimer's disease, *Trends Neurosci.*, 2003, **26**, 207-214.
10. A. Voegelin, S. Poster, A. C. Scheinost, M. A. Marcus and R. Kretzschmar, Changes in Zinc Speciation in Field Soil after Contamination with Zinc Oxide, *Environ. Sci. Technol.*, 2005, **39**, 6616-6623.
11. Y. P. Kumar, P. King and V. S. K. R. Prasad, Zinc biosorption on *Tectona grandis* L.f. leaves biomass: Equilibrium and kinetic studies, *Chem. Eng. J.*, 2006, **124**, 63-70.
12. A. Senthil Murugan, N. Vidhyalakshmi, U. Ramesh and J. Annaraj, A Schiff's base receptor for red fluorescence live cell imaging of Zn²⁺ ions in zebrafish embryos and naked eye detection of Ni²⁺ ions for bio-analytical applications, *J. Mater. Chem. B*, 2017, **5**, 3195-3200.
13. V. Kumar, U. Diwan, I. Sanskriti, R. K. Mishra and K. K. Upadhyay, A Categorical Naked-Eye Detection of Cu²⁺ and Zn²⁺ through a Donor-Acceptor-Donor (D-A-D)-Type Salicylaldimine: An Experimental and Theoretical Approach, *ChemistrySelect*, 2017, **2**, 11358-11363.
14. X. Lu, W. Zhu, Y. Xie, X. Li, Y. Gao, F. Li and H. Tian, Near-IR core-substituted naphthalenediimide fluorescent chemosensors for zinc ions: ligand effects on PET and ICT channels, *Chem. Eur. J.* 2010, **16**, 8355-8364.

15. Q. Q. Zhang, B. X. Yang, R. Sun, J. F. Ge, Y.J. Xu, N. J. Li and J. M. Lu, Development of a sensitive and selective fluorescent probe for Zn^{2+} based on naphthyridine schiff base, *Sens. Actuators B.*,2012,**1001**, 171–172.
16. M. Li, H.Y.Lu, R.L.Liu, J.D.Chen and C.F.Chen, Turn-On Fluorescent Sensor for Selective Detection of Zn^{2+} , Cd^{2+} , and Hg^{2+} in Water, *J. Org. Chem.*,2012, **77**,3670-3673.
17. X. Liu, N. Zhang, J. Zhou, T. Chang, C. Fanga and D. Shanguan, A turn-on fluorescent sensor for zinc and cadmium ions based on perylene tetracarboxylic diimide, *Analyst*, 2013, **138**, 901-906.
18. Z. Liu, C. Zhang, Y. Chen, F. Qian, Y. Bai, W. He and Z. Guo, *In vivo* ratiometric Zn^{2+} imaging in zebrafish larvae using a new visible light excitable fluorescent sensor, *Chem. Commun.*,2014,**50**, 1253-1255.
19. A Bhattacharyya, S Ghosh, SC Makhal and N Guchhait, Hydrazine bridged coumarin-pyrimidine conjugate as a highly selective and sensitive Zn^{2+} sensor: Spectroscopic unraveling of sensing mechanism with practical application, *Spectrochimica Acta Part A: Molecular Spectroscopy*, 2017, **183**, 306-311.
20. S. Nad, M. Kumbhakar and H.Pal, Photophysical Properties of Coumarin-152 and Coumarin-481 Dyes: Unusual Behavior in Nonpolar and in Higher Polarity Solvents, *J. Phys. Chem. A* 2003, **107**, 4808-4816.
21. L.Tang, Z. Huang, Z. Zheng, K. Zhong and Y. Bian, A new thiosemicarbazone-based fluorescence “turn-on” sensor for Zn^{2+} recognition with a large stokes shift and its application in live cell imaging, *J. Fluoresc.* 2016, **26**, 1535–1540.

22. M.Y. YUAN, D. N. ZHANG, H. F. YAN, W. H. Liu, D. F. Li and Y. Q. Zhang, Synthesis and Antibacterial Activity of *N*-(4-Substituted phenylthiazol-2-yl) coumarins, *Chin. J. Org. Chem.*, 2011, **31**, 1930-1933.
23. M.J. Frisch, et al., GAUSSIAN 03, Revision D.01, Gaussian, Inc., Wallingford, CT, 2004.
24. B.K. Paul, A. Samanta, S. Kar, N. Guchhait, Evidence for excited state intramolecular charge transfer reaction in donor-acceptor molecule 5-(4-dimethylamino-phenyl)-penta-2,4-dienoic acid methyl ester: Experimental and quantum chemical approach, *J. Lumin.* 2010, **130**, 1258–1267.
25. S. Dhar, D.K. Rana, S.S. Roy, S. Roy, S. Bhattacharya and S.C. Bhattacharya, Effect of solvent environment on the Photophysics of a newly synthesized bioactive 7-oxy(5-selenocyanato-pentyl)-2H-1-benzopyran-2-one, *J. Lumin.* 2012, **132**, 957–964.
26. E. Lippert, W. Luder, H. Boos, in: A. Mangini (Ed.) *Advances in Molecular Spectroscopy*, **443**, Pergamon Press, Oxford, 1962.
27. C. Reichardt, Solvatochromic Dyes as Solvent Polarity Indicators, *Chem. Rev.* 1994, **94**, 2319–2358.
28. S. Ghosh, A. Chakraborty, S. Kar and N. Guchhait, Constrained photophysics of partially and fully encapsulated charge transfer probe (E)-3-(4-Methylaminophenyl) acrylic acid methyl ester inside cyclodextrin nano-cavities: Evidence of cyclodextrins cavity dependent complex stoichiometry, *Spectrochimica Acta Part A: Molecular Spectroscopy*, 2010, **75**, 320–324.
29. S. Jana, S. Dalapati, S. Ghosh, S. Kar and N. Guchhait, Excited State Charge Transfer reaction with dual emission from 5-(4-dimethylamino-phenyl)-penta-2,4-dienitrile: Spectral

measurement and theoretical density functional theory calculation, *J. Mol. Struct.*, 2011, **998**, 136–143

30. A. Chakraborty, S. Kar, D. N. Nath and N. Guchhait, Photoinduced Intramolecular Charge Transfer Reaction in (*E*)-3-(4-Methylamino-phenyl)-acrylic Acid Methyl Ester: A Fluorescence Study in Combination with TDDFT Calculation, *J. Phys. Chem. A* 2006, **110**, 12089-12095.

31. J.R. Lakowicz, Principles of Fluorescence Spectroscopy (third ed.) Springer, New York, 2006.

32. IUPAC, Nomenclature, symbols, units and their usage in spectrochemical analysis—II. data interpretation Analytical chemistry division, *Spectrochim. Acta B*, 1978, **33**, 241–245.

33. P. Job, Formation and Stability of Inorganic Complexes in Solution, *Annali di Chimica Applicata.*, 1928, **9**, 113–203.

34. H.A. Benesi and J.H. Hildebrand, A Spectrophotometric Investigation of the Interaction of Iodine with Aromatic Hydrocarbons, *J. Am. Chem. Soc.*, 1949, **71**, 2703-2707.

35. F. Basolo and R. G. Pearson, Mechanisms of Inorganic Reactions, **47**, 1958, John Wiley and Sons, Inc., New York.

36. A. Bhattacharyya, S. Ghosh, S.C. Makhal and N. Guchhait, Hydrazine appended self assembled benzoin-naphthalene conjugate as an efficient dual channel probe for Cu²⁺ and F⁻: A spectroscopic investigation with live cell imaging for Cu²⁺ and practical performance for fluoride, *J. Photochem. Photobiol. A*, 2018, **353**, 488-498.

37. A. Bhattacharyya, S. C. Makhal, S. Ghosh, A. A. Masum and N. Guchhait, CHEF-Affected Fluorogenic Nanomolar Detection of Al³⁺ by an Anthranilic Acid–Naphthalene Hybrid: Cell Imaging and Crystal Structure, *ChemistrySelect*, 2017, **2**, 9924– 9929.

TOC

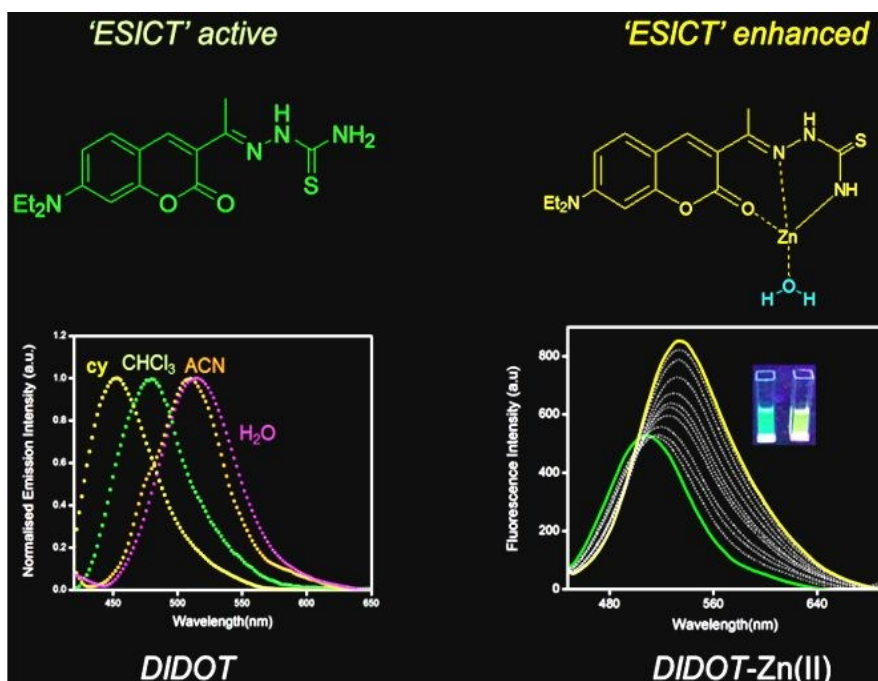
Establishing the merit of a coumarin-based thiosemicarbazone as an excited state intramolecular charge transfer probe: efficient Zn (II) mediated green to yellow emission swing

Arghyadeep Bhattacharyya, Subhash Chandra Makhal, and Nikhil Guchhait*

Department of Chemistry, University of Calcutta, 92, A.P.C. Road, Kolkata-700009, India

*Corresponding author. Tel.: +913323508386; fax: +913323519755.

E-mail address: nguchhait@yahoo.com (N. Guchhait).



Abstract: Novel coumarin based probe **DIDOT** has been synthesized and characterized. The charge transfer phenomenon in **DIDOT** is selectively enhanced by Zn (II) along with CHEF mechanism to afford emission swing from green to yellow. The limit of detection for Zn (II) is ~30 nM. Mechanism of Zn (II) detection has been delineated by theoretical and experimental studies. The practical utility has been explored by successful detection of Zn (II) in spiked water samples.